

**Preferred citation:** P.J. Mangin and P. Geoffroy. Printing roughness and compressibility: a novel approach based on ink transfer. In **Fundamentals of Papermaking**, *Trans. of the IXth Fund. Res. Symp. Cambridge, 1989*, (C.F. Baker & V. Punton, eds), pp 951–975, FRC, Manchester, 2018.  
DOI: 10.15376/frc.1989.2.951.

# **PRINTING ROUGHNESS AND COMPRESSIBILITY: A NOVEL APPROACH BASED ON INK TRANSFER**

P. J. Mangin and P. Geoffroy  
Pulp and Paper Research Institute of Canada,  
570 St. John's Boulevard, Pointe Claire, P.Q., Canada, H9R 3J9

## **ABSTRACT**

A new approach to characterize the roughness of paper in contact with ink under compression in the printing nip is proposed. The printing roughness is calculated from the parameters of the ink coverage function contained in the ink transfer equations. The approach assumes an identity between the ink transfer coverage function and the pore shape-function of the surface pores. Although the printing roughness correlates well with standard roughness/porosity tests, different regression lines result from different printing conditions. The printing roughness was found to be inversely linearly related to the logarithm of the printing pressure with the slope of the regression line representing a measure of the compressibility of the paper surface. The compressibility is independent of the printing pressure but, for rough papers, is a function of the nip dwell time.

## INTRODUCTION

During sheet compression in a printing nip, the thickness of the ink film on the printing plate required to contact and transfer to all of the exposed fiber surface depends on the smoothness of the paper surface contour (1). Therefore, *printing roughness* is defined as the roughness of paper in contact with ink, under compression in the printing nip. Parker (2,3) developed the 'Print-Surf' on the assumption that air-leak roughness measured with a backing similar to an offset press blanket was equivalent to some kind of printing roughness.

Print density (4,5) and the surface area covered by a drop of liquid ink (6) have also been used to define printing "smoothness". However, despite all these attempts, no method has yet been found to characterize a paper roughness as seen by the ink in a dynamic mode as it occurs in the printing nip. In other words, no true evaluation of a *dynamic* paper roughness in the printing nip has ever been established.

This paper proposes an approach to the characterization of the topography of paper in the printing nip using ink transfer data. The approach is similar to that of a previous paper (7) dealing with the characterization of uncompressed paper. From the analysis of ink transfer data, a pore shape function as well as a single roughness value that may truly be called 'printing roughness' are obtained.

## EXPERIMENTAL

### Paper Samples

An eastern Canadian newsprint containing 45% thermomechanical pulp, 35% stone groundwood, and 20% low yield sulfite was calendered to 4 smoothness levels in the PAPRICAN laboratory calender. The calendering conditions, basis weight, and bulk properties of the samples are listed in Table 1. Air-leak roughness and permeability, and the mean pore size of the samples are listed in Table 2.

Sample	Calendering Level*	Nip Load kN/m	Caliper $\mu\text{m}$	Bulk $\text{cm}^3/\text{g}$
1-0	0	Uncalendered	112	2.40
1-1	1	20	98	2.09
1-2	2	20,40	90.5	1.95
1-3	3	20,40,60	87	1.86
1-4	4	20,40,60,80	83.5	1.80

* Roll temperature:	50°C
Roll Peripheral Velocity:	50 m/min
Samples basis weight:	46.7 g/m <sup>2</sup>

Table 1. Calendering Conditions and Physical Properties.

## Printing

The 5 samples were printed at 4 printing pressures (1.8, 2.9, 3.6, and 4.4 MPa), and 5 printing speeds (1, 2, 3, 4 and 5 m/s) with an IGT-AIC2 Printability Tester. Samples were conditioned for 12 hours at 23°C and 50% relative humidity, and printing was done in a conditioned atmosphere. The GFL SCAN standard ink (8) was used. The amount of ink applied to the printing plate was varied between 0.5 and 12 g/m<sup>2</sup>, for a total of 12 ink weights on the printing plate for each printing condition. Ink transfer curves were fitted to the data using a modified version of the Walker-Fetsko ink transfer equation (9).

## THEORY

Our evaluation of printing roughness in a printing nip from ink transfer data is based on the mathematical identity between the expression of the ink transfer coverage function and the pore shape function of paper surface pores obtained from 3D profilometry data (7). Furthermore, as will be shown later, it is logical to assume some kind of analogy between

Sample	Parker Print-Surf Roughness $\mu\text{m}$		Bendtsen Smoothness mL/min	Sheffield Smoothness mL/min	Bristow Roughness $\mu\text{m}$	Air Permeability		Mean Pore Size ** $\mu\text{m}$
	S5	S20				Parker Print-Surf P20*	mL/min	
1-0	7.80	6.40	4.35	490	250	175	350	7.55
1-1	6.25	4.70	3.30	210	160	155	265	5.15
1-2	5.25	4.15	2.80	140	115	155	250	5.00
1-3	4.60	3.80	2.60	105	100	95	220	4.30
1-4	4.40	3.45	2.35	90	85	85	205	4.00

\* P20 is the air permeability measured with the Parker Print-Surf fitted with the air permeability head under a clamping pressure of 2 MPa (20 kgf/cm<sup>2</sup>).

\*\* measured with mercury intrusion.

Table 2. Paper Roughness and Porosity.

the ink progressively covering and filling-in paper surface pores and the 3D profilometry stylus sensing the inside contours of the same paper surface pores.

### Ink Transfer and Roughness Evaluation

Figure 1 shows the S-shaped curve characteristic of the change in ink transfer,  $Y$ , as the amount of ink on the printing plate,  $X$ , is increased. The fractional ink transfer,  $Y/X$ , is also shown. Many researchers have fitted the S-shape ink transfer curve to equations having three or four parameters. While the usefulness of these empirical ink transfer equations has been questioned (9, 10), De Grâce and Mangin (11, 12) used a mechanistic approach to show that ink transfer curve shapes resulted from the interaction between

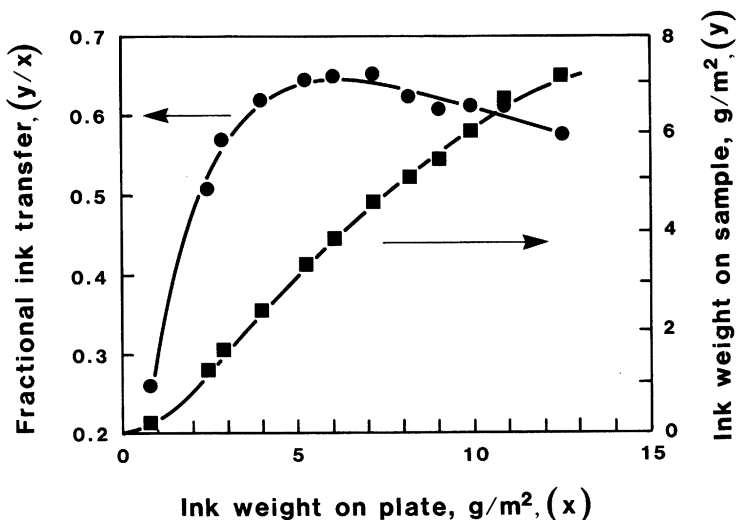


Figure 1. Ink transfer curve for the newsprint calendered at  $S10 = 4.70 \mu\text{m}$ . Printing conditions are: GFL ink, 3.60 MPa printing pressure, and 4 m/s printing speed. Fitting is performed on the fractional ink transfer curve (8).

press conditions, mainly printing speed, pressure, and ink viscosity, and paper properties, mainly roughness and porosity (11). They also showed that the first part of the ink transfer curve before the maximum in the fractional transfer (see Figure 1) was most sensitive to paper roughness (11), and to the rate of coverage of the paper surface by the ink. This is expressed by the coverage parameter contained in the ink transfer equations (9).

In Figure 2, the paper surface is represented by the Equivalent Surface Pore (7) obtained by the rotation of the pore shape function of paper. As shown in Figure 2, during ink transfer to paper, the ink contacts exposed paper surfaces and starts to fill-in the surface pores. As the

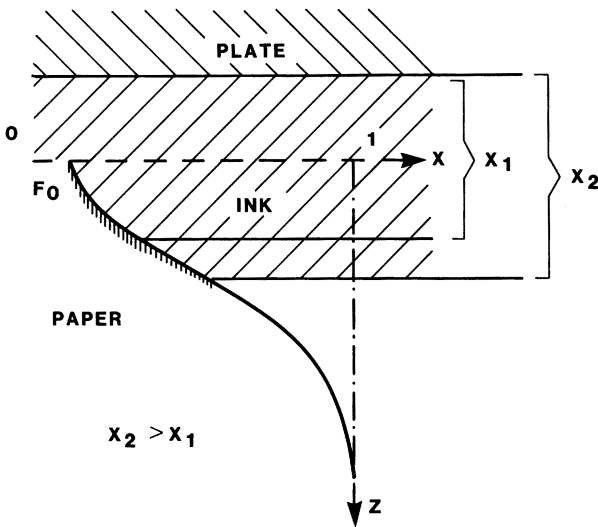


Figure 2. Schematic of ink filling-in of the paper surface represented by the Equivalent Surface Pore (ESP) (7). When the amount of ink on the plate is increased, the ESP is filled by ink and the contact between the conical sides of the pore and the ink increases accordingly.

ink weight (X) on the printing plate is increased, more and more of the paper surface is contacted, and more and more pores are filled-in with ink. Complete coverage of the paper surface by ink occurs close to the maximum in fractional ink transfer (11).

We assume that the coverage and filling-in of the surface pore by the ink is analogous to the action of a 3D profilometer stylus probing the paper surface. If an absolute paper roughness value could be defined, the value would be independent of the measuring technique, whether a stylus (profilometry method), air (air leak method), light (optical method), or ink (proposed method) was used to sense the paper surface. Therefore, differences in the roughness values from different methods are related to the testing conditions, compressed (static or dynamic) and/or uncompressed state of the paper surface, and whether a portion of the surface porosity is included or not in the evaluation (13, 14).

For instance, paper surface is not compressed during 3D profilometric evaluation. Profilometric roughness is limited by the pore size that can be sensed according to the stylus diameter. On the other hand, paper surface is compressed in a printing nip. Furthermore, ink does not have the same size limitations as the diameter stylus and can probe deeper pores.

#### Ink Transfer Coverage and Paper Surface Pore Shape Functions

The most common ink transfer equation is that derived by Walker and Fetsko (15):

$$Y = A(X) [bB(X) + f(X - bB(X))] \quad (1)$$

A(X) and B(X) are the ink coverage and the immobilization functions defined as follows:

$$A(X) = 1 - e^{-kX} \quad (2)$$

$$B(X) = 1 - e^{-X/b} \quad (3)$$

where X = ink weight on the printing plate before printing,  
 Y = ink weight transferred to the paper during printing,  
 f = splitting parameter,  
 b = immobilization or 'absorbency' parameter, and  
 k = coverage or 'smoothness' parameter.

Karttunen *et al.* (16) proposed the introduction of a "flattened fraction"  $F_0$ , i.e. the fraction of the paper surface in contact with an uninked plate. Mangin *et al.* (9) introduced a compression parameter  $\gamma$ . Both modifications were intended to correct deficiencies in the original Walker-Fetsko (WF) coverage function A(X). Combining these modifications, the coverage factor of the WF equation becomes:

$$A(X) = 1 - (1 - F_0)e^{-(kX)^\gamma} \quad (4)$$

As seen in Table 3, major modifications of the WF equation are derived from the above general equation by fixing different values of both the correction parameter  $\gamma$  and the flattened fraction  $F_0$ . In the general form proposed here to correct the coverage function of the WF equation, the parameters  $F_0$  and  $\gamma$  are functions of both the experimental printing conditions and paper properties.

It is readily apparent that the ink coverage equation (4) uses the *same mathematical expression* as the asymptotic regression law proposed (1) to represent the pore shape function  $F_1(z)$  of paper:

Authors referred	Reference Number	Parameter $F_0$	Parameter $\gamma$	Equation (in text)
Walker, Fetsko	(15)	$F_0 = 0$	$\gamma = 1$	(2)
Rupp, Rieche	(17)	$F_0 = 0$	$\gamma = 2$	(4)
Wultsch, Shubert	(18)	$F_0 = 0$	$\gamma = 3/2$	(4)
Karttunen et al.	(16)	$F_0$ variable	$\gamma = 1$	(4)
Mangin et al.	(9)	$F_0 = 0$	$\gamma$ variable	(4)
General form		$F_0$ variable	$\gamma$ variable	(4)

Table 3. Summary of Walker-Fetsko Based Ink Transfer Models (1).

$$F_1(z) = 1 - (1 - F_0) e^{-(k_1 z)} \quad (5)$$

with  $k_1 = k^\gamma$  (6)

and  $z = x^\gamma$  (7)

The pore shape function  $F_1(z)$  was derived from 3D profilometry evaluation assuming no paper compression and quasi-static conditions, while  $A(X)$  (equation 4) is obtained from the ink transfer equation *under dynamic printing conditions*.

Just as the pore shape function  $F_1(z)$  is used to calculate the paper roughness from 3D profilometry, the ink coverage function  $A(X)$  obtained from the ink transfer experiments can be used to calculate the printing roughness.

From the general equation of topography (Z)

$$G_{3,1} = \left[ \int_0^1 z^3 dF_1(z) \right]^{1/3} \quad (8)$$

and relation (5) representing the pore shape function, the paper roughness can be calculated as

$$G_{3,1} = \left[ k (1 - F_0) \int_0^{z_{\max}} z^3 e^{-kz} dz \right]^{1/3} \quad (9)$$

When second order terms are neglected, derivation and calculation of above expression provides a paper roughness value (Z) expressed as

$$G_{3,1} = \left[ \frac{6(1 - F_0)}{k^3} \right]^{1/3} \quad (10)$$

where  $k$  and  $F_0$ , the parameters describing the pore shape function of paper without compression, are obtained from 3D profilometry data.

By analogy, from the general ink coverage function (4), considering the changes of parameters in equations (6) and (7), and above relation (10) expressing the paper roughness, the printing roughness  $R_g$  is given by:

$$R_g = \left[ \frac{6(1 - F_0)}{k^3 \gamma} \right]^{1/3} \quad (11)$$

where  $k$  and  $F_0$ , and  $\gamma$ , the parameters describing the pore shape function of paper in the printing nip, are obtained from ink transfer data, and equations (1), (3) and (4).

It should however be noted that the asymptotic regression law  $F_1(z)$  is used as an approximation to the Gaussian distribution of paper surface pores (7). Similarly, a Gaussian distribution of surface pores was implied by Ichikawa *et al.* (19). They proposed a model based on the WF equation where both the coverage  $A(X)$  and the immobilization  $B(X)$  functions were represented by cumulative normal distribution functions. However, due to its complexity and large number of parameters (6), the Ichikawa ink transfer model was never properly used or recognized. For all practical applications, it has been shown (7) that the asymptotic regression law could be used with an equivalent degree of success.

## RESULTS AND DISCUSSION

The ink transfer data and the printing roughness of the samples examined under different printing conditions are shown in Appendix. The printing roughness has been calculated from equation (11), with  $F_0 = 0$ . For some ink transfer curves (8 out of 100), convergence on a set of 4 parameters ( $k$ ,  $b$ ,  $f$ , and  $\gamma$ ) could not be obtained and the parameter  $\gamma$  had to be given a fixed value of 1.

## Correlations

Correlations between the proposed printing roughness and conventional air-leak roughness, air permeability, and porosity (measured by mercury intrusion) are shown in Table 4. All the grand mean determination coefficients from correlations between the printing roughness  $R_g$  and other common roughness and porosity values are above 0.90. It should however be noted that the uncalendered samples are not included in the regression analysis.

According to the pore shape function, surface pores of an uncalendered paper are very large ( $Z$ ), more open to the paper surface than pores of a calendered paper. Progressive calendering of the paper gradually closes the surface pores, i.e. it reduces the pore size. The closing of surface pores in the first calender nip (calendering level 1) is more important than in later nips. This "closing" effect is supported by the significantly bigger difference, 1.70  $\mu\text{m}$ , in air-leak roughness between the uncalendered sample and the first nip calendered sample compared to subsequent roughness reductions, only 0.40  $\mu\text{m}$  in average, in the second to fourth calendering nips (Table 2). Similarly, when an uncalendered paper is printed, the closing of the surface pores due to the printing pressure is more important than for calendered papers. This is shown in Figure 3 where the printing roughness obtained at 4 different printing pressures is plotted as a function of the S20 Parker Print-Surf roughness. The experimental uncalendered sample roughness is lower than the one calculated from the regression lines.

The good correlation obtained between the Parker Print-Surf and the printing roughness shows that the Parker Print-Surf can be used as an indicator of printing roughness when the printing pressure is fixed. However, different regression lines correspond to different printing pressures meaning, as expected from the definition of printing roughness, that printing roughness is a function of printing pressure.

Test	Printing Pressure, MPa					Grand Mean
	1.79	2.86	3.60	4.40		
S5	$\bar{X}$	0.9482	0.9055	0.8571	0.8942	0.9012
	SD	0.0462	0.0884	0.1306	0.1151	0.1054
S10	$\bar{X}$	0.9720	0.9095	0.8512	0.8982	0.9114
	SD	0.0182	0.0770	0.0615	0.0584	0.0709
S20	$\bar{X}$	0.9608	0.9397	0.8580	0.9001	0.9146
	SD	0.0362	0.0542	0.0593	0.0764	0.0703
Bendsten	$\bar{X}$	0.9421	0.9233	0.8889	0.8865	0.9102
	SD	0.0575	0.0722	0.0795	0.1174	0.0870
Sheffield	$\bar{X}$	0.9372	0.9482	0.8555	0.8782	0.9047
	SD	0.0574	0.0461	0.1095	0.1107	0.0945
P20*	$\bar{X}$	0.9444	0.7922	0.7964	0.8943	0.8568
	SD	0.4444	0.1292	0.1326	0.0536	0.1183
Mean Pore Size**	$\bar{X}$	0.8949	0.7045	0.7386	0.8514	0.7973
	SD	0.0700	0.1462	0.1719	0.0789	0.1471

$\bar{X}$ , SD are the mean and standard deviation of regressions corresponding to the 5 printing speeds, uncalendered sample not included.

\* air permeability Parker Print-Surf.

\*\* measured by mercury intrusion.

Table 4. Determination Coefficient  $R^2$  of Correlation Between Printing Roughness and Common Roughness/Porosity Indices.

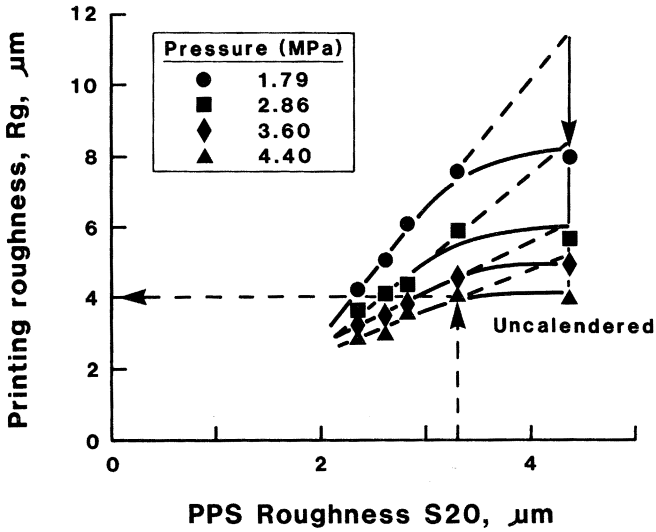


Figure 3. The printing roughness as a function of the S20 Parker Print-Surf roughness for 4 printing pressures. Points shown are the average of printing roughness measured at the 5 printing speeds (1, 2, 3, 4 and 5 m/s).

Figure 3 also shows that the change in printing roughness with air leak roughness becomes much less as printing pressure goes up. For instance, at 1.79 MPa and for the 5 printing speeds, the printing roughness decreases from 8.5  $\mu\text{m}$  (uncalendered) to 4.35  $\mu\text{m}$  (calendering level 4), while at 4.40 MPa, it only varies from 3.95  $\mu\text{m}$  to 2.95  $\mu\text{m}$ . Furthermore, Figure 3 shows that Parker Print-Surf S20 values of 2.25, 2.55, 2.85 and 3.25  $\mu\text{m}$  will all result in the same printing roughness ( $R_g = 4.0 \mu\text{m}$ ) when printed at 1.79, 2.86, 3.6 and 4.4 MPa, respectively. The levelling off of printing roughness with increased printing pressure explains the printers common practice of increasing printing pressure when printing rough papers. These results also explain why paper roughness was found not be an important quality

parameter in offset printing (20, 21). These conclusions would be similar with the Bendtsen and Sheffield air-leak roughness.

### Effect of Printing Speed on the Printing Roughness

For all calendering levels and printing pressures, the printing speed, within the range and the samples studied, was found to have virtually no influence on the printing roughness. This implies that the flow velocity of the ink within the surface pores should be independent of the printing speed. Furthermore, it verifies former conclusions that changes in ink transfer with printing speed are mainly due to modifications in the ink film splitting behavior (12).

### Effect of Printing Pressure on the Printing Roughness

Figure 4 shows that the printing roughness decreases with the printing pressure. As expected, the paper appears smoother to an ink film when the printing pressure is increased. When an ink film is brought into contact with a paper surface under increasing printing pressure two effects occur as far as the paper surface is concerned. First, as seen before, paper pores close, resulting in a reduction of the printing roughness. Second, ink penetration in the porous paper increases, resulting in an increase in printing roughness. However, it can be verified from the Hagen-Poiseuille law that the ink flow velocity in a porous medium varies as a function of the printing pressure and the square of the surface pore size (derivation is presented elsewhere (22)). Therefore, when pressure is increased, surface pore size will decrease more rapidly than the ink flow velocity, resulting in a decreased pore penetration by ink, and so a lower printing roughness.

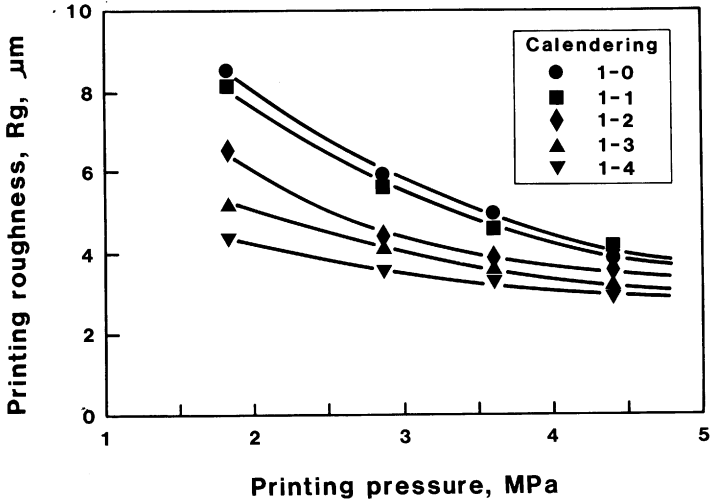


Figure 4. The printing roughness as a function of the printing pressure. Points shown are the average of printing roughness measured at the 5 printing speeds (1, 2, 3, 4 and 5 m/s).

#### Surface Compressibility of Paper in a Printing Nip

The variation of printing roughness with printing pressure can be used to evaluate the compressibility of paper in a printing nip. The reduction  $K$  in roughness  $R$  as a function of the pressure  $P$  is used to define the paper surface compressibility (23, 24, 25):

$$K = -dR/dP \quad (12)$$

Figure 4 shows that the printing roughness does not vary linearly as a function of the printing pressure. Therefore, the compressibility parameter  $K$  is a function of the printing pressure itself. However, Table 5 shows that the printing roughness  $R_g$  is linearly related to  $\log P$  with an average determination coefficient  $R^2$  of 0.9553 as

$$R_g = R_1 + K' \log P \quad (13)$$

$R_1$  is the printing roughness corresponding to  $P = 1$  MPa ( $\log P = 0$ ).

Sample	Determination Coefficient $R^2$		Compressibility Coefficient $K'$	
	Mean*	SD	Mean*	SD
1-0	0.9382	0.0534	10.90	1.2
1-1	0.9824	0.0156	10.95	1.6
1-2	0.9402	0.0430	7.95	1.4
1-3	0.9388	0.0382	5.45	1.1
1-4	0.9762	0.0279	3.45	0.4
Grand Mean	0.9553	0.0427	-	-

\* mean of 5 printing speeds

Table 5. Determination Coefficients of Correlation Between the Printing Roughness and the Printing Pressure Logarithm.

It then becomes possible, as proposed by Bristow (25), to define a compressibility parameter  $K'$  independent of the pressure applied as

$$K' = -dR/d(\log P) \quad (14)$$

According to equations (13) and (14), the compressibility parameter  $K'$  is not a function of the printing pressure. However, although paper compressibility is expected to be a function of the nip dwell time (24, 26), the relationship between the compressibility parameter and nip dwell time is not readily apparent. Regression analysis shows the compressibility parameter  $K'$  to be independent of the printing speed, except for the uncalendered paper where  $K'$  decreased with increasing speed. The relationship between

the nip dwell time (0.8 to 4 ms) at each printing speed (1 to 5 m/s) and the compressibility of calendered newsprints in a printing nip becomes apparent in Figure 5 where the printing roughness is plotted as a function of the S10 roughness of the paper. The slope of the regression lines is a function of the printing speeds. This shows that some relationship between nip dwell time and compressibility should only be expected for rough and compressible papers.

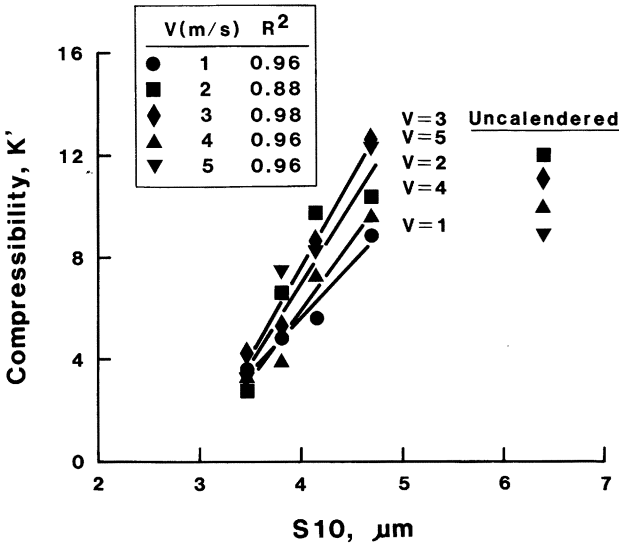


Figure 5. The printing compressibility parameter  $K'$  as a function of the S10 roughness of the newsprint samples.

Furthermore, as expected from the common understanding that rougher paper is more compressible, the compressibility parameter  $K'$  is shown in Figure 5 to increase linearly with increasing paper roughness. Therefore, the compressibility parameter  $K'$  is a function of the paper and compression times (i.e. printing speed) in the printing nip.

## CONCLUSIONS

A novel evaluation of printing roughness - the roughness of paper under actual printing conditions - is proposed. The printing roughness is calculated from ink transfer curves by identification of the ink coverage function with the pore shape-function of the Equivalent Surface Pore.

Although the printing roughness correlates well with standard roughness/porosity tests, different regression lines result from different printing conditions.

The printing roughness was found to be linearly related to the logarithm of the printing pressure. The slope of the regression line yields a compressibility parameter  $K'$ , which is independent of printing pressure, but is a function of the paper structure and of the nip dwell times.

## ACKNOWLEDGEMENTS

The authors wish to thank S. Smallwood for calendering the newsprint samples, S. Sauriol for the mercury intrusion evaluations, and the Physical Analysis Section for other sample testing.

## REFERENCES

1. De Grâce, J.H., and Dalphond, J.E., The Development of Print Density and Print Through in Newsprint, to be published in TAGA Proceedings (1989).
2. Parker, J.R., An Air-Leak Instrument to Measure Printing Roughness of Paper and Board, Paper Technology, 6(2), 126-130 (1965).
3. Parker, J.R., The Measurement of Printing Roughness, TAPPI 64 (12):56-58 (1981).
4. O'Neil, J.R., The Printing Smoothness of Paper. A New Method of Measurement, APPITA, 201-206, May (1959).
5. Walker, W.C. and Carmack, R.F., The Printing Smoothness of Paper, Adv. in Printing Science and Techn., W.H. Banks Ed., Pentech Press, London, Vol. 3, 203-219 (1964).
6. Van Der Vloodt, P.C., A New Method for Measuring the Surface Roughness of Paper, Ibid, Vol. 3, 191-202 (1964).
7. Mangin, P.J., The Measurement of Paper Roughness: A 3D Profilometry Approach, PPR 708, October 1988.
8. SCAN P35:72, Test Printing of Newsprint in the GFL Rotary Test Printing Press, Scandinavian Pulp, Paper and Board Testing Committee (1972).
9. Mangin, P.J., Lyne, M.B., Page, D.H. and De Grâce, J.H., Ink Transfer Equations. Parameters Estimation and Interpretation, Adv. in Printing Science and Techn., W.H. Banks Ed., Pentech Press, London, Vol. 16, 180-205 (1982).
10. Mangin, P.J., A Discussion of the Usefulness of Ink Transfer Equations, TAPPI Proc., Printing and Reprography Conf., Chicago, Il., 143 (1980).

11. De Grâce, J.H. and Mangin, P.J., A Mechanistic Approach to Ink Transfer. Part I: Effect of Substrate Properties and Press Conditions, *Ibid* 9, Vol. 17, 312-322 (1984).
12. De Grâce, J.H. and Mangin, P.J., A Mechanistic Approach to Ink Transfer. Part II: The Splitting Behavior of Inks in Printing Nip, *Ibid* 9, Vol. 19, 146-161 (1988).
13. Bekk, J., Horizontal Porosity with the Bekk Smoothness Tester As It Affects Smoothness, *Paper Trade Journal* 63rd year, TAPPI Section, 217-219, 1934.
14. Mangin, P.J. and De Grâce, J.H., An Analysis of the Accuracy of Measuring Paper Roughness with the Parker Print-Surf, *TAPPI Proc.*, Printing and Graphic Arts/Testing Conf., Niagara Falls, N.Y., U.S.A., 125-134, 1984.
15. Walker, W.C. and Fetsko, J.M., A Concept of Ink Transfer During Printing, *American Ink Maker*, 33, No. 12, 38 (1955).
16. Karttunen, S., Kautto, H. and Oittinen, P., New Modifications of Ink Transfer Models, *Proceedings Eleventh Conference IARIGAI*, Canadaigua, N.Y., U.S.A., 33-52 (1971).
17. Rupp, E., und Rieche, K., Beiträge zur Bedruckarbeit von Papier und Volien, *Inst. Grafische Technik*, Leipzig (1959).
18. Wultsch, F., und Schubert, K., Untersuchungen verschiedener Papiersorten mit dem Fogra-bedruckbarkeitsgerät, *Das Papier*, 13 (23/24), 600-607 (1959).
19. Ichikawa, I., Sato, K. and Ito, Y., A New Concept of Ink Transfer Equation, *Res. Bull. Govern., Printing Bureau, Japan*, No. 1 (1962).
20. Lyne, M.B., Multidimensional Scaling of Print Quality, *TAPPI* 62 (11):103 (1979).

21. Lyne, M.B., Parush, A., Richer, F., Jordan, B.D., Donderi, D.C. and Ramsay, J.O., A Multidimensional Analysis of Paper-Related Factors in the Subjective Evaluation of Print Quality, Trans. 7th Research Symposium, Cambridge (1981).
22. Mangin, P.J., Etude de la déstructuration de la surface du papier en zone d'impression offset, Thèse de l'Institut National Polytechnique de Grenoble, France, 310 pp., Octobre 1988.
23. Bristow, J.A. and Ekman, H., Paper Properties Affecting Gravure Print Quality, TAPPI 64 (10):115-118 (1981).
24. Bristow, J.A., The Surface Compressibility of Paper - A Printability Property, Ibid 9, Vol. 15, 373-383 (1979).
25. Bristow, J.A., The Surface Compressibility of Paper, STFI, Stockholm, Sweden, 19 p., May 11, 1981.
26. Watanabe, K. and Amari, T., Dynamic Compressive Modulus of Paper, Reports on Progress in Polymer Physics in Japan, Vol., XXV, 409-412.

## APPENDIX

## INK TRANSFER PROPERTIES AND PRINTING ROUGHNESS

Sample	Printing Speed m/s	Printing Pressure MPa	k	$\gamma$	$y/x_{\max}$	$x_{\max}$ g/m <sup>2</sup>	$Y_{\max}$ g/m <sup>2</sup>	$R_g$ $\mu\text{m}$
1-0	1.0	1.79	0.2006	1.000*	0.7675	15.61	11.98	9.058
1-0	2.0	1.79	0.2065	1.000*	0.6943	10.76	7.473	8.801
1-0	3.0	1.79	0.2151	1.0305	0.6583	10.75	7.076	8.853
1-0	4.0	1.79	0.2161	0.9551	0.6352	11.49	7.031	7.849
1-0	5.0	1.79	0.1833	0.8679	0.6202	10.71	6.640	7.922
1-0	1.0	2.86	0.2736	0.9582	0.8149	11.20	9.129	6.291
1-0	2.0	2.86	0.2934	0.9714	0.7552	10.63	8.027	5.981
1-0	3.0	2.86	0.3300	0.9356	0.7016	9.040	6.343	5.128
1-0	4.0	2.86	0.2908	0.9200	0.6728	8.735	5.877	5.660
1-0	5.0	2.86	0.2707	0.8311	0.6532	8.476	5.536	5.384
1-0	1.0	3.60	-	-	-	-	-	-
1-0	2.0	3.60	0.3594	0.8331	0.7833	10.16	7.954	4.263
1-0	3.0	3.60	0.3091	1.000*	0.7486	8.056	6.030	5.879
1-0	4.0	3.60	0.3418	0.9544	0.7096	7.453	5.288	5.062
1-0	5.0	3.60	0.4037	1.0322	0.6785	7.136	4.842	4.635
1-0	1.0	4.40	0.4413	0.8941	0.8535	11.59	9.893	3.776
1-0	2.0	4.40	0.3946	0.7499	0.8007	9.067	7.259	3.649
1-0	3.0	4.40	0.4245	0.9437	0.7522	7.436	5.594	4.079
1-0	4.0	4.40	0.4285	0.8690	0.7237	6.725	4.867	3.795
1-0	5.0	4.40	0.4589	1.1904	0.7001	5.885	4.120	4.593
1-1	1.0	1.79	0.2390	1.000*	0.6917	9.241	6.392	7.602
1-1	2.0	1.79	0.2292	1.000*	0.6397	8.338	5.334	7.930
1-1	3.0	1.79	0.3241	1.3825	0.5982	7.076	4.232	8.626
1-1	4.0	1.79	0.3399	1.3720	0.5748	6.928	3.982	7.987
1-1	5.0	1.79	0.3368	1.4644	-	-	-	8.943
1-1	1.0	2.86	0.3218	1.000*	0.7336	8.724	6.400	5.646
1-1	2.0	2.86	0.3066	1.000*	0.6887	7.404	5.099	5.926
1-1	3.0	2.86	0.4105	1.2673	0.6394	6.330	4.047	5.616
1-1	4.0	2.86	0.3647	1.1819	0.6228	6.252	3.894	5.987
1-1	5.0	2.86	0.4177	1.4033	0.6013	5.663	3.406	6.187

Sample	Printing Speed m/s	Printing Pressure MPa	k	$\gamma$	$y/x_{\max}$	$x_{\max}$ g/m <sup>2</sup>	$Y_{\max}$ g/m <sup>2</sup>	$R_g$ $\mu\text{m}$
1-1	1.0	3.60	0.4043	1.1409	0.7552	8.584	6.482	5.106
1-1	2.0	3.60	0.3825	0.9354	0.7086	7.124	5.048	4.465
1-1	3.0	3.60	0.4145	1.0552	0.6775	6.160	4.174	4.603
1-1	4.0	3.60	0.3787	1.0027	0.6481	6.110	3.960	4.811
1-1	5.0	3.60	0.3670	0.8385	0.6254	6.028	3.770	4.211
1-1	1.0	4.40	0.4862	1.1077	0.7652	8.425	6.447	4.040
1-1	2.0	4.40	0.3912	0.8437	0.7238	7.049	5.102	4.012
1-1	3.0	4.40	0.4216	0.8108	0.6920	6.257	4.329	3.660
1-1	4.0	4.40	0.3838	0.8967	0.6605	6.211	4.102	4.289
1-1	5.0	4.40	0.3572	0.8277	0.6443	6.139	3.955	4.260
1-2	1.0	1.79	0.3305	1.0213	0.6723	7.914	5.321	5.629
1-2	2.0	1.79	0.3342	1.2530	0.6264	6.821	4.273	7.174
1-2	3.0	1.79	0.3555	1.3054	0.5983	5.888	3.523	7.011
1-2	4.0	1.79	0.3272	1.1257	0.5803	6.068	3.521	6.390
1-2	5.0	1.79	0.3375	1.2250	0.5668	5.893	3.340	6.875
1-2	1.0	2.86	0.3755	0.7925	0.7255	7.828	5.679	3.950
1-2	2.0	2.86	0.4063	0.9038	0.6726	6.423	4.320	4.101
1-2	3.0	2.86	0.4565	1.1706	0.6401	5.369	3.437	4.550
1-2	4.0	2.86	0.3683	0.9063	0.6159	5.842	3.598	4.493
1-2	5.0	2.86	0.3825	1.0626	0.5965	5.660	3.376	5.046
1-2	1.0	3.60	0.4528	0.9322	0.7446	7.109	5.293	3.803
1-2	2.0	3.60	0.3948	0.6553	0.6966	6.942	4.835	3.341
1-2	3.0	3.60	0.4584	1.1012	0.6645	5.332	3.543	4.289
1-2	4.0	3.60	0.3676	0.7644	0.6326	6.034	3.817	3.905
1-2	5.0	3.60	0.4167	0.9336	0.6206	5.329	3.308	4.115
1-2	1.0	4.40	0.4958	0.9041	0.7602	7.047	5.358	3.427
1-2	2.0	4.40	0.5089	1.0206	0.7107	5.609	3.986	3.620
1-2	3.0	4.40	0.4887	0.9639	0.6867	5.252	3.607	3.623
1-2	4.0	4.40	0.4530	0.8636	0.6632	5.281	3.502	3.600
1-2	5.0	4.40	0.4304	0.8471	0.6344	5.246	3.328	3.711
1-3	1.0	1.79	0.3055	0.8158	0.6802	7.514	5.111	4.781
1-3	2.0	1.79	0.3750	1.0599	0.6279	5.880	3.692	5.139
1-3	3.0	1.79	0.3630	1.0526	0.5962	5.694	3.395	5.280
1-3	4.0	1.79	0.3219	0.8855	0.5765	5.872	3.385	4.957
1-3	5.0	1.79	0.3846	1.2795	0.5711	5.236	2.990	6.171

Sample	Printing Speed m/s	Printing Pressure MPa	k	$\gamma$	$y/x_{\max}$	$x_{\max}$ g/m <sup>2</sup>	$Y_{\max}$ g/m <sup>2</sup>	$R_g$ $\mu\text{m}$
1-3	1.0	2.86	0.4208	1.0080	0.7241	6.374	4.615	4.348
1-3	2.0	2.86	0.3943	0.9401	0.6749	5.933	4.004	4.359
1-3	3.0	2.86	0.4045	0.9317	0.6385	5.525	3.528	4.223
1-3	4.0	2.86	0.4206	0.9166	0.6170	5.075	3.312	4.020
1-3	5.0	2.86	0.3756	0.8319	0.5980	5.380	3.217	4.104
1-3	1.0	3.60	0.4729	0.8091	0.7442	6.656	4.953	3.331
1-3	2.0	3.60	0.4742	0.8834	0.7024	4.485	3.853	3.512
1-3	3.0	3.60	0.4822	0.8794	0.6670	5.026	3.352	3.451
1-3	4.0	3.60	0.4568	0.7858	0.6408	5.029	3.223	3.363
1-3	5.0	3.60	0.4601	0.9925	0.6235	4.723	2.944	3.927
1-3	1.0	4.40	0.5480	0.8002	0.7560	6.292	4.757	2.941
1-3	2.0	4.40	0.5285	0.7610	0.7161	5.457	3.908	2.952
1-3	3.0	4.40	0.5334	0.9217	0.6863	4.771	3.274	3.243
1-3	4.0	4.40	0.5335	1.0831	0.6613	4.424	2.926	3.588
1-3	5.0	4.40	0.5037	1.2551	0.6399	4.584	2.933	3.223
1-4	1.0	1.79	0.3476	0.7982	0.6726	7.123	4.791	4.224
1-4	2.0	1.79	0.3658	0.8132	0.6193	5.949	3.684	4.117
1-4	3.0	1.79	0.3320	0.8197	0.5877	4.834	3.429	4.487
1-4	4.0	1.79	0.3659	0.8740	0.5710	5.272	3.010	4.376
1-4	5.0	1.79	0.4110	1.017	0.5664	4.918	2.785	4.487
1-4	1.0	2.86	0.4641	0.8088	0.7123	6.409	4.565	3.381
1-4	2.0	2.86	0.4630	0.8326	0.6605	4.484	3.623	3.450
1-4	3.0	2.86	0.3975	0.7351	0.6348	5.525	3.507	3.580
1-4	4.0	2.86	0.4600	0.8896	0.6128	4.702	2.881	3.626
1-4	5.0	2.86	0.4255	0.8533	0.5946	4.815	2.863	3.768
1-4	1.0	3.60	0.5006	0.8994	0.7378	6.061	4.472	3.386
1-4	2.0	3.60	0.5353	0.8951	0.6895	4.975	3.430	3.179
1-4	3.0	3.60	0.5151	0.9097	0.588	4.698	3.095	3.323
1-4	4.0	3.60	0.5345	0.9733	0.6382	4.282	2.733	3.343
1-4	5.0	3.60	0.5454	1.0243	0.6169	4.077	2.524	3.381
1-4	1.0	4.40	0.6032	0.7732	0.7421	5.932	4.402	2.686
1-4	2.0	4.40	0.5359	0.8051	0.7126	5.243	3.683	3.003
1-4	3.0	4.40	0.5597	0.7251	0.6722	4.690	3.152	2.768
1-4	4.0	4.40	0.5328	0.8488	0.6484	4.451	2.886	3.101
1-4	5.0	4.40	0.5234	0.8904	0.6359	4.324	2.749	3.234

\* Gamma fixed

## Transcription of Discussion

# **PRINTING ROUGHNESS AND COMPRESSIBILITY: A NOVEL APPROACH BASED ON INK TRANSFER**

P. J. Mangin and P. Geoffroy

### **ERRATA**

Table 2, page 954, 7th. column (Bristow Roughness) should read 17.5, 15.5, 15.5, 9.5 and 8.5 (i.e. values are divided by 10).

### **Dr. I.K. Kartovaara Finnish Pulp and Paper Institute**

A few years back I was confronted with exactly the same problem as you. How to describe mathematically the cumulative roughness curve obtained with a profilometric instrument. After trying several curves, including the normal distribution, on a large number of samples I ended up with exactly the same result as you, that the logistics curve gave by far the best fit to all the very different samples.

### **Dr. P.J. Mangin**

Thankyou for your comment, I have to add something here. When I was working on ink transfer analysis some years ago we analysed the ink transfer equation proposed by Ichikawa et al., They used a log-normal function to describe the ink transfer curves. At the time we thought that the log-normal equation was too complex, but in hindsight, perhaps it was the correct one. Unfortunately trying to calculate and find the solutions to this type of equation can be quite complex that is why there is always an approximation used.

### **Dr.H.L. Baumgarten PTS Munich**

I have just one short question, do you have any idea how you may relate your results to the printability in gravure printing?

### **Dr. P.J. Mangin**

I am afraid not.

**Dr. J. R. Parker**

Having discussed this work with Dr. Mangin, I believe that we are in agreement that some caution must be exercised in applying this interesting approach. Whilst seeming to be critical I must point out that probing the paper surface with ink is the only method available to us for finding out with some degree of reality how the paper surface is seen by the ink in the nip of a printing press. By careful use of this approach it should be possible to get estimates not only of the effective roughness but also the shape of the paper surface with which the ink makes contact during impression. The results from ink transfer studies are critically dependent on the assumptions made about the ink transfer process. These affect the values obtained both for the ink coverage and for the corresponding depth of the ink penetration. Unfortunately, few attempts have been made to verify such results by, for example, measuring ink coverage by direct observation.

In the present paper I must, for three different reasons, question the validity of equation (11) from which the roughness,  $R_g$ , has been calculated. The influence of  $\delta$  is the opposite of what might be expected, its dimensions do not balance, and the physical basis of the underlying assumptions are not clear.

The  $\delta$  quantity is used in the ink transfer equation to modify the shape of the exponential curve of the ink coverage function to obtain an improved fit to experimental data. It is not unreasonable to assume that observed variations in  $\delta$  correspond to variations in the relative proportions of deep and shallow surface pores. When similar exponential expressions are used to represent pore depth distributions, there can be no doubt that  $\delta$  has this meaning. Fig 'A' below shows the effect of  $\delta$  on the shape of the depth distribution curve, the range of  $\delta$  chosen being rather less than that for the current results. It is important to note that as  $\delta$  increases, the proportion of shallow pores decreases.

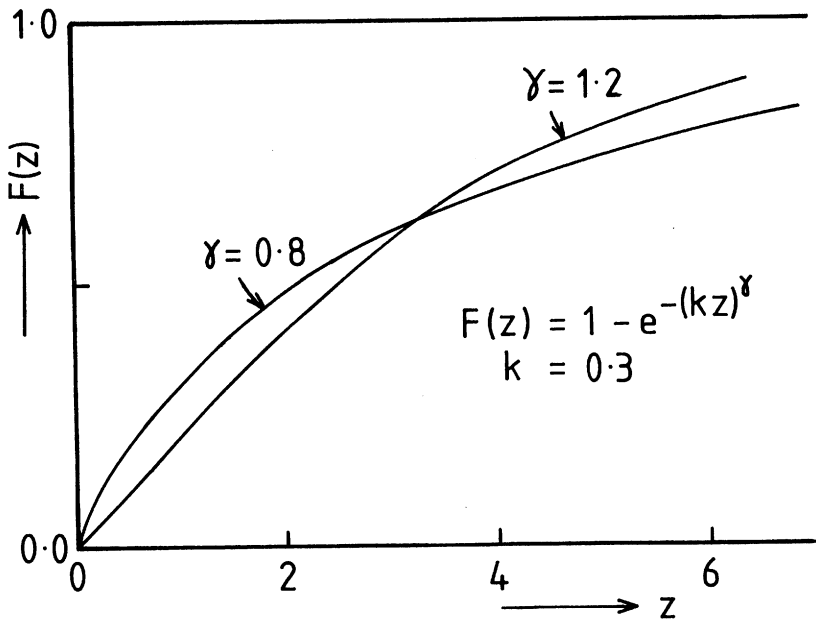


Fig. A

Examples of cumulative pore depth distributions calculated from the modified exponential formula.

Suppose that a print is made by pressing paper against a smooth metal plate covered with a thin film of viscous ink of thickness  $x$ . The appearance of the resulting print seen under a microscope often strongly suggests that the ink has piled up to some increased depth  $z$  around each of the high spots in the paper surface, having been squeezed out of the contact areas. See Figure 'B'. The proportion of the paper surface wetted by the ink will depend this final depth  $z$ , so the relationship between  $A(x)$  and  $z$ , rather than  $x$ , gives the pore depth distribution  $F(z)$ .

The relationship between  $z$  and  $x$  will depend on the extent to which the displaced ink redistributes itself within the non-contact areas of the printing plate. Hsu (1) assumed that all the displaced ink was immediately and uniformly redistributed throughout the non-contact areas. In contrast, it is implicit in the Walker-Fetsko equation that the depth of the ink in the non-contact areas is unaffected when a print is made. This is illustrated in Fig 'B'. For each assumption it is possible to calculate the relationship of  $z$  to  $x$  from the shape of the ink coverage function, thus obtaining a pore depth distribution. In his paper, Dr Mangin seems to assume the  $z$  is equal to  $x$ , without explaining the fate of the displaced ink. The resulting depth distribution function is of course strongly affected by the assumption made.

The difficulty with the dimensions centres on the smoothness parameter  $k$  which occurs in the ink coverage function:

$$A(x) = 1 - \exp\{-(kx)^\delta\}$$

Ink thickness  $x$  must have the dimension length, so  $k$  must be reciprocal length. Similarly,  $z$  is also a length, so that any  $k$  associated with it is again reciprocal length. From the equation of topography, (8),  $Rg$  must also be a length. Equation (11) can be written:

$$Rg = (1/k)^\delta [6(1-F_0)]^{1/\delta}$$

so that, unless  $\delta$  is one the dimensions are unbalanced.

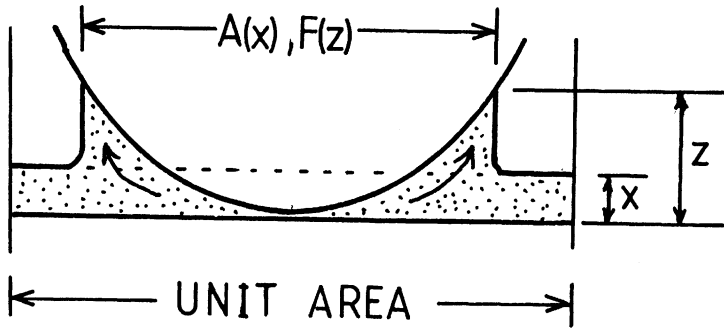


Fig. B

A diagrammatic representation of a paper surface, above, in contact with a printing plate, showing a possible effect of the displaced ink on ink film thickness.

As a check, and also to indicate the effects of these errors on the results presented in the paper, I calculated values of the cube-root-mean-cube roughness  $R_g$  for comparison with values of  $R_g$  given by equation (11, starting from the same assumptions as Mangin:

$$\begin{aligned} z &= x \\ F_0 &= 0 \\ F(z) &= 1 - \exp\{ -(kz)^\delta \} \end{aligned}$$

Values for  $R_3$  were then obtained by numerical integration of the equation of topography, as suggested in Fig 'C'. Thus:

$$\begin{aligned} R_3^3 &= \int_0^1 z^3 dF(z) \\ &= \int_0^\infty (1-F(x)) d(z^3) \\ &= 3 \int_0^\infty z^2 \cdot e^{-(kz)^\delta} \cdot dz \end{aligned}$$

Choosing a value for  $k$  of 0.3, similar to the average for Mangin's results, I obtained the value shown in the following table:

$\delta$	$R_g$ Equation (11)	$R_3$ Numerical Integration
1.2	7.71	4.97
0.8	4.76	8.50

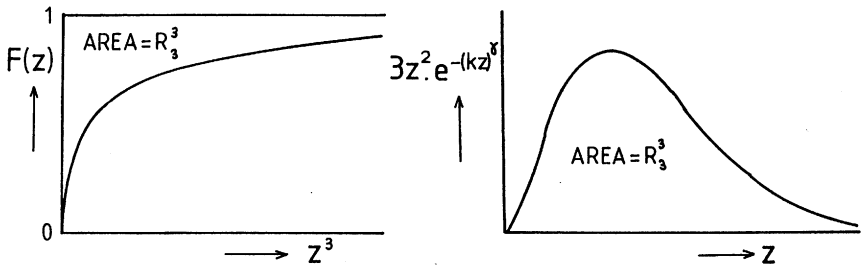


Fig. C

Calculation of  $R_3$  from a pore depth distribution for the general case, left and right for a surface with a modified exponential depth distribution.

As I remarked previously, increases in  $R_s$  indicate a fall in the proportion of deeper pores in the paper surface, so that  $R_s$  should decrease as shown here as  $R_s$  increases. If this is so then the errors I have pointed out will radically affect the results presented in Figs 3-5 of Dr Mangin's paper.

REFERENCE

- (1) Hsu, Bay-Sung, Distribution of depressions in the paper surface: a method of determination, Brit. J. of Appl. Phys., 13, 155-158 (1962).

Dr. P.J. Mangin

The roughness equation proposed as equation (9) integrates as:

$$G_s^3 = \underbrace{\frac{6(1-F_0)}{K^3 \delta}}_{\text{PART I}} - \underbrace{(1-F_0)e^{-(kz_{\text{max}})\delta} P(z_{\text{max}}\delta)}_{\text{PART II}}$$

The actual 3D roughness, from which all calculations are made, is Part I of the equation. The terms corresponding to Part II are neglected. They are a function of the maximum depth at which ink has penetrated the paper surface. Now, if you ever printed on newsprint, you will realise that this simplification is valid as ink penetration is usually of 20  $\mu\text{m}$  or more. Therefore,  $P(z_{\text{max}}\delta)$ , which is a polynomial of the third order, times the exponential is small compared to the roughness (Part I). Roughness remains the important term, and the polynomial is crossed out. So the actual printing roughness is a useful approximation. These points were discussed in detail with Dr John Parker outside the meeting.

As far as the differences between the numerical (provided by John Parker's contribution) and the literal values (given by equation 11 of the presentation) are concerned, I checked both John Parker's calculations and my own, and both are mathematically correct. So it seems that the two methods can provide very different results. This should be further analysed and resolved. However, I must add that I do not favour that too much emphasis be put on the use of the exponent  $\delta$ . The exponent is a fiddle factor used to find solutions to ink transfer parameters. If it could be avoided altogether, there would be no problem, and both

methods would give identical results. Actually, Dr Parker is reading more into the physical significance of  $\gamma$  than I had myself imagined. And I thank him for evoking this possibility because there may be something into this. At present my data do not allow me to put any true physical meaning (paper pore shape, for instance, as proposed by Dr Parker) to  $\gamma$ .

Furthermore, the printing roughness  $R_g$  is quite sensitive to this exponent  $\gamma$ . This is related to the fact that  $\gamma$  is incorporated as an exponential of an exponential function. Around values of  $q$ , the variation of printing roughness related to  $\gamma$  is rapid, and the differences between the two methods obtained at 0.8 and 1.2 are clear.

Last but not least, when using the Marquardt's compromise to converge on a solution for the ink transfer parameters, you find that the parameters  $k$  and  $\gamma$  are not independent. In other words, when  $\gamma$  varies,  $k$  varies accordingly. This solves the dimension problems because what is considered as the pore shape factor is  $k$ . Mathematically,  $\gamma$  is always varying (let us say between 0.8 and 1.2) but  $k$  has units of  $\mu\text{m}^{-1}$ .

You need to separate physics from pure mathematical problems related to convergence on a solution. With this in mind, and outside the extreme values of  $\gamma$ , I forecast the John Parker's calculations and mine should be in good agreement, ie printing roughness values should correlate well. In conclusion, I would like to thank John Parker very much for his contribution and for pointing out this specific problem.